

# GALERKIN LEAST-SQUARES APPROXIMATIONS FOR HERSCHEL-BULKLEY FLUID FLOWS THROUGH AN AXISYMMETRIC ABRUPT EXPANSION

**Fernando Machado, [fmachado@mecanica.ufrgs.br](mailto:fmachado@mecanica.ufrgs.br)**

**Flávia Zinani, [fla@mecanica.ufrgs.br](mailto:fla@mecanica.ufrgs.br)**

**Sergio Frey, [frey@mecanica.ufrgs.br](mailto:frey@mecanica.ufrgs.br)**

Laboratory of Applied and Computational Fluid Mechanics (LAMAC)  
Mechanical Engineering Department, UFRGS  
Rua Sarmento Leite, 425 – 90059-170 – Porto Alegre, RS, Brazil.

**Abstract.** *The study of non-Newtonian fluid flows in expansions is of great interest for researchers in the several branches of engineering, due to their wide application both in industry and academy. The objective of this paper is to simulate flow problems involving a viscoplastic fluid through an axisymmetric abrupt expansion. The mechanical model employed is based on the mass and momentum conservative equations for isochoric flows coupled with the Generalized Newtonian Liquid constitutive equation, with the Papanastasiou-regularized Herschel-Bulkley viscosity function. The mechanical model is approximated by a stabilized finite element scheme, namely the Galerkin Least-squares method. This method (GLS) is used in order to overcome the numerical difficulties of the classical Galerkin method: the Babuška-Brezzi condition and the inherent instability in advective flow regions. The method is built adding mesh-dependent terms in order to increase the stability of the classical Galerkin formulation without damaging its consistency. The GLS formulation is applied to study the influence of shear-thinning and yield stress in the flow dynamics of Herschel-Bulkley fluids through an axisymmetric 1:4 expansion. Problems involving mild Reynolds numbers, for a Herschel-Bulkley number range between 0 and 100 are presented. The results are physically comprehensive and are in accordance with the literature. A physical analysis is performed.*

**Keywords:** *viscoplastic fluid; Herschel-Bulkley; finite elements; Galerkin least-squares; abrupt expansion flow.*

## 1. INTRODUCTION

Among non-Newtonian fluids, a class called viscoplastic fluids represents a group which has a special interest for researchers, due to possessing several applications in different sections in engineering. Such fluids seem to behave as rigid solids when subjected to shear stress smaller than a yield stress, and when submitted to greater levels of stress, they behave as viscous fluids, usually presenting viscosity shear-thinning. In fact, these fluids behave as extremely viscous materials when subjected to low stress, and suffer an abrupt change in behavior when the stress attains the yield stress, beginning to behave as mild viscous fluids (Souza Mendes and Dutra, 2004). Examples of viscoplastic materials are: molten chocolate, polymer melts and solutions, pharmaceutical products, among others (Schramm, 2006). In the literature, many models have been proposed in order to characterize viscoplasticity, usually in the form of a non-smooth function for the shear-stress. These models may be written in terms of a viscosity function, which is then employed beneath a generalized Newtonian constitutive equation. The Herschel-Bulkley model is one of the most employed viscosity functions. In numerical approximations, its regularized versions are usually employed instead of the classical model, in order to use a smooth viscosity function for the whole flow domain.

Recent publication (Jay et al., 2001) employed the finite element method to simulate flows of viscoplastic fluids through a sudden axisymmetric expansion, employing the Herschel-Bulkley and Bingham models approximated by the bi-viscosity model. They analyzed the influence of shear-thinning, inertia and yield stress values on the structure of the flow and on pressure and head losses. The authors also compared numerical and experimental results. Burgos et al. (1999) analyzed flows of regularized Herschel-Bulkley models such as Papanastasiou (1987), the bi-viscosity (Lipscomb and Denn, 1984) and Bercovier and Engelman (1984) for three-dimensional flows, concluding that all models are equivalent in predicting the yield surface provided a proper choice of regularization parameters. Alexandrou et al. (2001) studied steady flows of Herschel-Bulkley fluids in a canonical three-dimensional expansion with aspect ratio 1:2 and 1:4, employing a mixed-Galerkin finite element formulation. The results reveal the strong interplay between the Bingham and Reynolds numbers and their influence on the formation and break up of stagnant zones in the corner of the expansion and on the size and location of plug flow.

In the numerical approximation context, the classical Galerkin method for incompressible fluids suffers from two difficulties: the need to satisfy the Babuška-Brezzi condition (Ciarlet, 1978) in order to employ a compatible combination of velocity and pressure subspaces, and the inherent instability of central difference schemes in the approximation of advective dominated flows (Brooks and Hughes, 1982). The Galerkin least-squares method (GLS), introduced for Stokes equations in (Hughes et al. 1982), has been developed to enhance the stability of the original Galerkin method, by adding mesh-dependent terms to the Galerkin formulation, which are functions of the residuals of

Euler-Lagrange equations evaluated element wise. Since the residuals of the Euler-Lagrange equations are satisfied by the exact solutions, consistency is preserved in these methods. This methodology was also extended to incompressible Navier-Stokes equations in (Franca and Frey, 1992), preserving the capability to circumvent Babuška-Brezzi condition and to generate stable approximations even for highly advective flows.

The main goal of the present work is to employ a Galerkin least-squares formulation to approximate the flow dynamics of a Herschel-Bulkley fluid through an axisymmetric 4:1 expansion. With this purpose, we employ a Papanastasiou (1987) regularized version of the Herschel-Bulkley equation. We study the arisen of unyielded zones of two kinds: stagnation zones in the corner of the expansion and rigid body motion zones around the symmetry axis both upstream and downstream the expansion. We vary parameters as the yield stress and the power-law index and perform a sensibility analysis of how these parameters affect the topology of the yield surface and the flow dynamics.

## 2. MECHANICAL MODELING

The mechanical modeling that we concern is constituted of the laws of mass and momentum balance, and a constitutive equation for the stress.

### 2.1. Mass Conservation

The mass conservation principle for or system  $\Omega$  with boundary  $\Gamma$ , states that the mass variation in a volume  $\Omega$  is equal to the net mass flow rate in  $\Omega$  (Slattery, 1999):

$$\frac{\partial}{\partial t} \int_{\Omega} \rho d\Omega + \int_{\Gamma} \rho \mathbf{u} \cdot \mathbf{n} d\Gamma = 0 \quad (1)$$

where  $\rho$  is the mass density, and  $\mathbf{u}$  is the velocity vector. The differential form of Eq.(1) is obtained using Reynolds transport theorem and a localization argument (Gurtin, 1981):

$$\frac{\partial \rho}{\partial t} + \text{div}(\rho \mathbf{u}) = 0 \quad (2)$$

If we assume that the flow is isochoric, Eq.(2) reduces to:

$$\text{div } \mathbf{u} = 0 \quad (3)$$

### 2.2. Momentum balance

For a system of body and surface forces ( $\mathbf{b}$ ,  $\mathbf{t}$ ), the momentum balance may be expressed by Cauchy's theorem (Gurtin, 1981): "a necessary and sufficient condition for the momentum balance laws to be satisfied is that a stress tensor field  $\mathbf{T}$  exists such that:

- a)  $\mathbf{T}=\mathbf{t}\mathbf{n}$ , where  $\mathbf{n}$  is the outward unit vector,
- b)  $\mathbf{T}$  satisfies the motion equation:

$$\rho \left( \frac{\partial \mathbf{u}}{\partial t} + [\text{grad } \mathbf{u}] \mathbf{u} \right) = \text{div } \mathbf{T} + \mathbf{b} \quad (4)$$

- c)  $\mathbf{T}$  is symmetric.

### 2.3. Material behavior

The form of the stress tensor  $\mathbf{T}$  is given by a constitutive equation. Here we assume that  $\mathbf{T}$  obeys the Generalized Newtonian Liquid (GNL) model, i.e.:

$$\mathbf{T} = -p\mathbf{I} + 2\eta(\dot{\gamma})\mathbf{D} \quad (5)$$

where  $p$  is the hydrostatic pressure,  $\mathbf{I}$  is the unit tensor,  $\mathbf{D}$  is the strain rate tensor,  $\eta$  is the viscosity function, which is dependent of  $\dot{\gamma}$ , the magnitude of  $\mathbf{D}$  ( $\dot{\gamma}=(\text{tr}\mathbf{D}^2)^{1/2}$ ) (Slattery, 1999). For Newtonian fluids,  $\eta$  is a constant viscosity function and it is denoted by  $\mu$ .

All fluids whose behavior differ from the ideal Newtonian one are called non Newtonian. Probably the most important feature of non Newtonian fluids is the fact that they present a shear-rate dependent viscosity (Bird et al., 1987). The viscosity functional dependence on the shear rate allows us to classify variable viscosity fluids as pseudoplastic, viscoplastic or dilatant.

Pseudoplastic fluids are those which viscosity decreases with an increase in shear rate. Dilatant fluids are those which viscosity increases with an increase in the shear rate. Viscoplastic fluids behave as extremely viscous materials when subjected to low shear stresses. When the stress attains a certain minimum level, called yield stress (denoted by  $\tau_0$ ), their viscosity suffers a sudden drop, and as the shear stress continues to increase, these materials behave as Newtonian or pseudoplastic fluids (Barnes, 1992; Souza Mendes and Dutra, 2004). Examples of viscoplastic fluids are: pastes, food products (Jay et al, 2001), colloidal suspensions, used thoroughly of the industry of the petroleum, plastic propellant doughs (Burgos and Alexandrou, 1999), greases and cement pastes (Schramm, 2006).

There are many constitutive models that aim to describe viscoplastic behavior. They are usually formulated as non-smooth viscosity functions, and they are built in order to accommodate empirical flow curves of shear stress versus shear rate. As examples of viscoplastic models we have the Bingham plastic, the Herschel-Bulkley and the Casson models (Barnes, 1992). The Herschel-Bulkley equation is one of the most employed viscoplastic model. It employs three rheological parameters: the yield stress  $\tau_0$ , the consistency index  $K$  and the power-law index  $n$ . The Herschel-Bulkley model for the shear stress may be stated as:

$$\begin{cases} \tau = \tau_0 + K\dot{\gamma}^n & \text{if } \tau > \tau_0 \\ \dot{\gamma} = 0 & \text{if } \tau \leq \tau_0 \end{cases} \quad (6)$$

where  $\tau$  is the shear stress and  $\dot{\gamma}$  the shear rate in viscometric flow. If  $n=1$  this function reduces to the classical Bingham plastic equation.

In numerical approximations, Eq. (6) poses the difficulty of possessing a discontinuous character. This difficulty may be overcome employing a regularization of the model. The most common regularization techniques are the bi-viscosity approximation (Lipscomb and Denn, 1984) and the Papanastasiou's regularization (Papanastasiou, 1987). The latter is the one employed in the present paper, in the form of a continuous viscosity function, which is valid for the whole stress range (both below and above  $\tau_0$ ):

$$\eta(\dot{\gamma}) = K\dot{\gamma}^{n-1} + \frac{\tau_0}{\dot{\gamma}}(1 - \exp(-\alpha\dot{\gamma})) \quad (7)$$

where  $\alpha$  is the regularization parameter. As  $\alpha$  grows, Papanastasiou's regularized model mimics the original model Herschel-Bulkley model, as it may be observed in the  $\tau$  versus  $\dot{\gamma}$ , showed in the Fig.1 below:

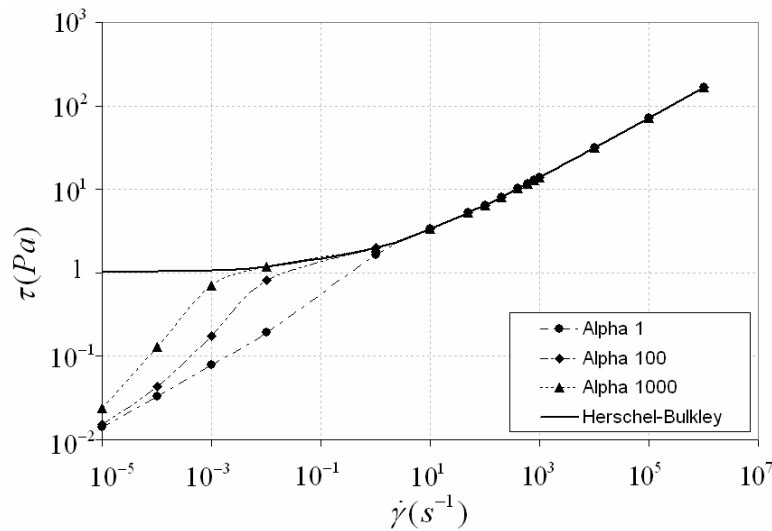


Figure 1. Shear stress as a function of shear rate as predicted by Eq. 7.

We employ Papanastasiou's regularization of Eq. (7) for the viscosity function in the GNL equation (Eq. (5)).

### 3. FINITE ELEMENT APPROXIMATION

In this section, a Galerkin least-squares (GLS) formulation (see, for instance, Zinani and Frey, 2006) for isochoric flows of generalized Newtonian fluids is presented.

The boundary value problem defined by the laws of mass conservation (Eq. (3)) and momentum balance for a generalized Newtonian liquid (Eq. (5)), plus the boundary conditions of prescribed velocity and forces is given by:

$$\begin{aligned}
 \operatorname{div} \mathbf{u} &= 0 && \text{in } \Omega \\
 \rho[\operatorname{grad} \mathbf{u}] \mathbf{u} &= -\operatorname{grad} p + \operatorname{div}(2\eta(\dot{\gamma})\mathbf{D}) + \mathbf{b} && \text{in } \Omega \\
 \mathbf{u} &= \mathbf{u}_g && \text{on } \Gamma_g \\
 (-p\mathbf{I} + 2\eta(\dot{\gamma})\mathbf{D})\mathbf{n} &= \mathbf{t}_h && \text{on } \Gamma_h
 \end{aligned} \tag{8}$$

where  $\Omega$  is the problem domain and  $\Gamma$  the boundary of  $\Omega$ , with  $\Gamma_g$  the portion of  $\Gamma$  where Dirichlet conditions are imposed and  $\Gamma_h$  the portion of  $\Gamma$  where Neumann conditions are imposed.

The usual approximation spaces for fluid dynamics were employed to define the finite element subspaces for velocity ( $\mathbf{V}^h$  and  $\mathbf{V}_g^h$ ) and pressure ( $P^h$ ) fields, over a partition  $C_h$  of the problem domain  $\bar{\Omega}$  parameterized by a characteristic mesh size  $h$ ,

$$\begin{aligned}
 P^h &= \{p \in C^0(\Omega) \cap L_0^2(\Omega) \mid p|_{\Omega_K} \in R_l(\Omega_K), \Omega_K \in C_h\} \\
 \mathbf{V}^h &= \{\mathbf{v} \in H_0^1(\Omega)^{nsd} \mid \mathbf{v}|_{\Omega_K} \in R_k(\Omega_K)^{nsd}, \Omega_K \in C_h\} \\
 \mathbf{V}_g^h &= \{\mathbf{v} \in H^1(\Omega)^{nsd} \mid \mathbf{v}|_{\Omega_K} \in R_k(\Omega_K)^{nsd}, \Omega_K \in C_h, \mathbf{v} = \mathbf{u}_g \text{ on } \Gamma_g\}
 \end{aligned} \tag{9}$$

Based on the approximation spaces of Eqs. (9), a Galerkin least-squares formulation for the non linear boundary value problem defined by Eq. (8) may be stated as: Find the pair  $(\mathbf{u}^h, p^h) \in \mathbf{V}_g^h \times P^h$  such as:

$$B(\mathbf{u}^h : \mathbf{u}^h, p^h; \mathbf{v} : \mathbf{u}^h, q) = F(\mathbf{v} : \mathbf{u}^h, q), \quad \forall (\mathbf{v}, q) \in \mathbf{V}^h \times P^h \tag{10}$$

where

$$\begin{aligned}
 B(\mathbf{u} : \mathbf{u}, p; \mathbf{v} : \mathbf{u}, q) &= \int_{\Omega} \rho[\operatorname{grad} \mathbf{u}] \mathbf{u} \cdot \mathbf{v} \, d\Omega + \int_{\Omega} 2\eta(\dot{\gamma})\mathbf{D}(\mathbf{u}) \cdot \mathbf{D}(\mathbf{v}) \, d\Omega - \int_{\Omega} p \operatorname{div} \mathbf{v} \, d\Omega - \int_{\Omega} q \operatorname{div} \mathbf{u} \, d\Omega + \\
 &+ \sum_{\Omega_K \in C_h} \int_{\Omega_K} (\rho[\operatorname{grad} \mathbf{u}] \mathbf{u} + \operatorname{grad} p - 2 \operatorname{div}(\eta(\dot{\gamma})\mathbf{D}(\mathbf{u}))) \cdot (\tau(\operatorname{Re}_K)\rho([\operatorname{grad} \mathbf{v}] \mathbf{u} - 2 \operatorname{div}(\eta(\dot{\gamma})\mathbf{D}(\mathbf{v})) - \operatorname{grad} q)) \, d\Omega_K
 \end{aligned} \tag{11}$$

$$F(\mathbf{v} : \mathbf{u}, q) = \int_{\Omega} \mathbf{f} \cdot \mathbf{v} \, d\Omega + \int_{\Gamma} \mathbf{t} \cdot \mathbf{v} \, d\Gamma + \sum_{\Omega_K \in C_h} \int_{\Omega_K} \mathbf{f} \cdot (\tau(\operatorname{Re}_K)(\rho[\operatorname{grad} \mathbf{v}] \mathbf{u} - 2 \operatorname{div}(\eta(\dot{\gamma})\mathbf{D}(\mathbf{v})) - \operatorname{grad} q)) \, d\Omega_K \tag{12}$$

with the stability parameter  $\tau$  being the same as in Franca and Frey, 1992, for the linear Newtonian fluid

$$\tau(\operatorname{Re}_K) = \frac{h_K}{2|\mathbf{u}|_p} \xi(\operatorname{Re}_K) \quad \text{with} \quad \xi(\operatorname{Re}_K) = \begin{cases} \operatorname{Re}_K, & 0 \leq \operatorname{Re}_K < 1 \\ 1, & \operatorname{Re}_K \geq 1 \end{cases} \quad \text{and} \quad \operatorname{Re}_K = \frac{\rho h_K |\mathbf{u}|_p}{2\eta(\dot{\gamma})} \tag{13}$$

where  $h_K$  stands for the  $K$ -element size,  $\operatorname{Re}_K$  the grid Reynolds number and the  $|\cdot|_p$  the  $p$ -norm on  $\mathcal{R}^{nsd}$ .

The solution of Eqs. (10)-(12) is performed via Gaussian quadrature for the approximation of the integrals, and a Newton's method for the solution of the non-linear system, formed after the variables are substituted by their expansions in shape functions (see Zinani and Frey, 2006).

## 4. NUMERICAL RESULTS

All computations were carried out by a finite element code for non-linear fluids – NNFEM – under development in the Laboratory of Computational and Applied Fluid Mechanics (LAMAC/UFRGS).

### 4.1. Flow over a backward-facing step

For the validation of the code NNFEM and an implementation for a Newtonian flow problem; we generated a two-dimensional mesh of 1,656 Q1/Q1 elements with 1,825 nodes to approximate flows over a step. The backward-facing step is a classic benchmark for fluid dynamics codes. Figure 2 gives an idea of the problem statement.

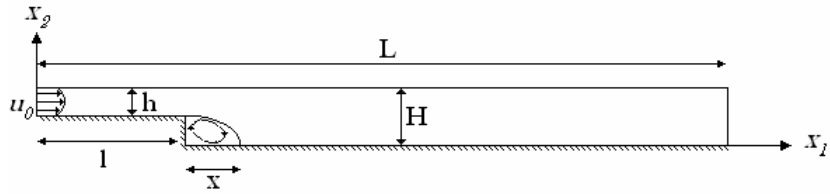


Figure 2. Problem statement for the backward-facing step.

We adopted the conditions of non-slip and impermeability at the walls, a horizontal parabolic velocity profile at the flow inlet, with mean velocity  $u_0=1\text{m/s}$ , and free traction at the flow outlet. The dimension of the step is defined by lengths  $L=13$  and  $l=3$  and heights  $H=1$  and  $h=0.5$ .

The Reynolds number is defined by:

$$\text{Re} = \frac{\rho 1.5 u_0 (H - h)}{\mu} \quad (14)$$

where  $\rho$  and  $\mu$  are the fluid's density and viscosity, respectively.

We compared our results with those presented in a GAMM workshop (*Gesellschaft für Angewandte Mathematik und Mechanik*), (Morgan, Periaux and Thomasset, 1982), where some researchers have carried out a comparison of the reattachment length of the flow downstream the step. Table 1 elucidates the methods used for the authors and the reattachment lengths found, comparing with those obtained in the present work, with the dimensionless reattachment length is scaled as  $d=x/(H-h)$ :

Table 1. Reference, method and results for the reattachment length (Morgan, Periaux and Thomasset, 1982).

Work	Method	$Re=50$ $d$ reattachment	$Re=150$ $d$ reattachment
<b>Present work</b>	FEM - $\mathbf{u}, p$	2.0	4.7
Kueny-Binder	Experimental	2.1	4.5
Dhatt-Hubert	FEM - $\mathbf{u}, p$	1.0	5.0
Donea-Giuliani, Laval	FEM - $\mathbf{u}, p$	2.0	5.0
Ecer-Rout-Ward	FEM - Chebsch method	2.0	4.7
Glowinsky et al.	FEM - $\mathbf{u}, p$	2.8	4.4
Hecht	FEM - streamlines	1.8	4.6
Macedo	FEM - $\mathbf{u}, p$	2.1	4.4

From Table 1, one may observe that the results obtained with NNFEM were in good agreement with the literature. For a more details on the validation of the code, see Zinani and Frey, 2006.

In Fig. 3, we depict the streamlines for the results of flows of Reynolds number equal 50 and 150, showing the growth of the recirculation as  $Re$  increases. This happens because, when the flow is more advective, i.e., for the higher  $Re$ , the inertia forces are too high and it takes a greater distance to promote the reattachment of the boundary layer downstream the step.

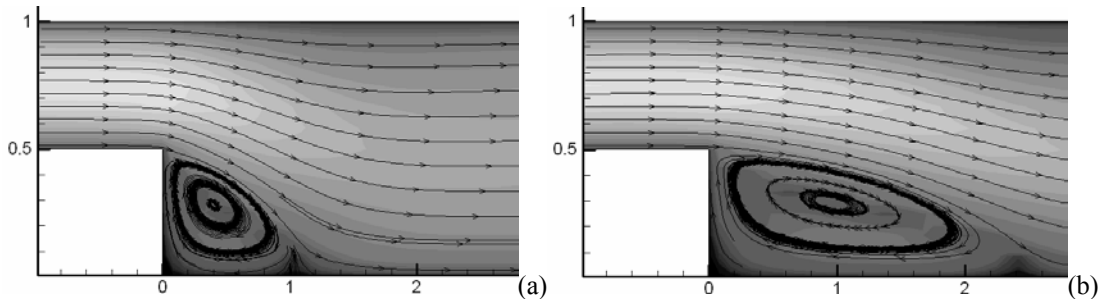


Figure 3. Recirculation downstream the expansion step, for (a)  $Re=50$  and (b)  $Re=150$ .

#### 4.2. Flow trough an axisymmetric expansion

The geometry studied herein is an axisymmetric 4:1 abrupt expansion. The inlet channel has length  $L_0$  and radius  $R_0$ , the outlet channel has length  $L_1$  and radius  $R_1$ . The ratios  $L_0/R_0 = 30$  and  $L_1/R_0 = 75$  were employed to assure fully

development of the flow. We adopted the conditions of non-slip and impermeability at the walls, a horizontal parabolic velocity profile at the flow inlet, with mean velocity  $u_0=1\text{m/s}$ , and free traction at the flow outlet.

The problem statement is depicted in Fig. 4 (a). After a mesh-dependency study, we have chosen a mesh with 16,236 nodes and 15,825 elements. To obtain precise results for stagnation zones and vortex formation, the mesh is highly refined near the expansion corner (Fig. 4 (b)).

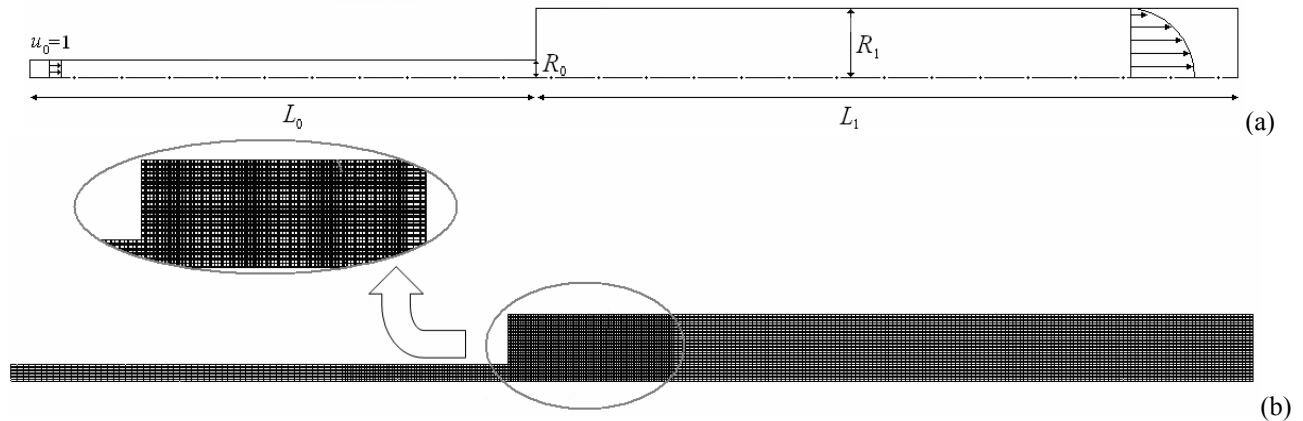


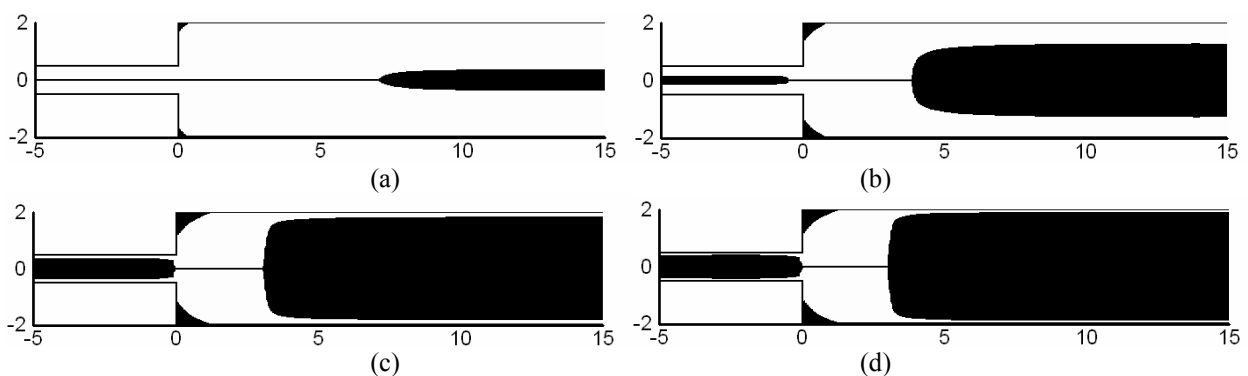
Figure 4. (a) Problem statement, (b) mesh employed: 16,236 nodes and 15,825 elements.

The flow of viscoplastic fluids possesses two distinct flow dynamics regime: yielded and unyielded zones. The unyielded zones occur where the stress is smaller than the fluid's yield stress. In such regions, the strain rates tend to zero. The remaining regions are called yielded zones. In these regions the fluid flows as a viscous material. The limit between yielded and unyielded zones is called yield surface. In the case of a Papanastasiou regularized model, its position is determined through the von Mises criteria, i.e., the stress is post-processed from the approximated velocity field and compared with the yield limit of the fluid.

In the following sections, we present pictures of the flow structure in terms of yielded and unyielded zones. The unyielded zones are plotted in black, and the yielded zones in white. We investigate the influence of varying the yield stress limit and power-law index, for a fixed negligible Reynolds number, in the position of the yielded surface. In the case of the flow in an expansion, two distinct unyielded zones tend to arise: one in the corner after the expansion, due to very low velocity values and gradients, and other along the symmetry axis, where strain rates and stresses are small, forming a plug-flow. The dimensionless pressure, radius, Reynolds and Herschel-Bulkley numbers are defined as:

$$p^* = \frac{p - p_0}{\rho u_0^2 / L}, \quad \text{Re} = \frac{\rho u_0 D_0 / 2}{K \left( \frac{u_0}{D_0 / 2} \right)^{n-1}}, \quad \text{Hb} = \frac{\tau_0}{K \left( \frac{u_0}{D_0 / 2} \right)^n}, \quad r = \frac{x_2}{D_0} \quad (15)$$

In Fig. 5, it is possible to examine the influence of the Herschel-Bulkley number,  $Hb$ , in the formation of unyielded zones in the expansion corner and in the symmetry axis. The  $Hb$  was varied from  $Hb=0.1$  to  $Hb=100$ . The power-law index was taken as  $n=0.37$ .



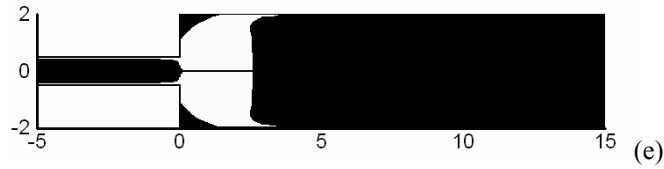


Figure 5. Yielded and unyielded regions,  $n=0.37$ , (a)  $Hb=0.1$ , (b)  $Hb=1$ , (c)  $Hb=10$ , (d)  $Hb=20$ , (e)  $Hb=100$ .

It is possible to perceive that as  $Hb$  increases, the size of the unyielded zones increase, due to the increasing yield stress. As below the yield stress the strain rates tend to zero, the unyielded zones form a plug-flow region along the symmetry axis, where the fluid flow with no shear rate between the flow layers. The plug-flow may be evidenced if we plot the axial velocity  $u^*=u_1/u_0$  versus the tube radius,  $r=x_2/D_0$  in a fully developed flow location, as in Fig. 6 (a), for the position  $x_1=10D_0$ . In Fig. 6 (b) we plot the pressure drop ( $\log(p^*)$ ) along the symmetry axis for the various fluids. It is clear that the formation of the unyielded plug-flow increases the pressure drop considerably, due to the high resistance to flow that it causes.

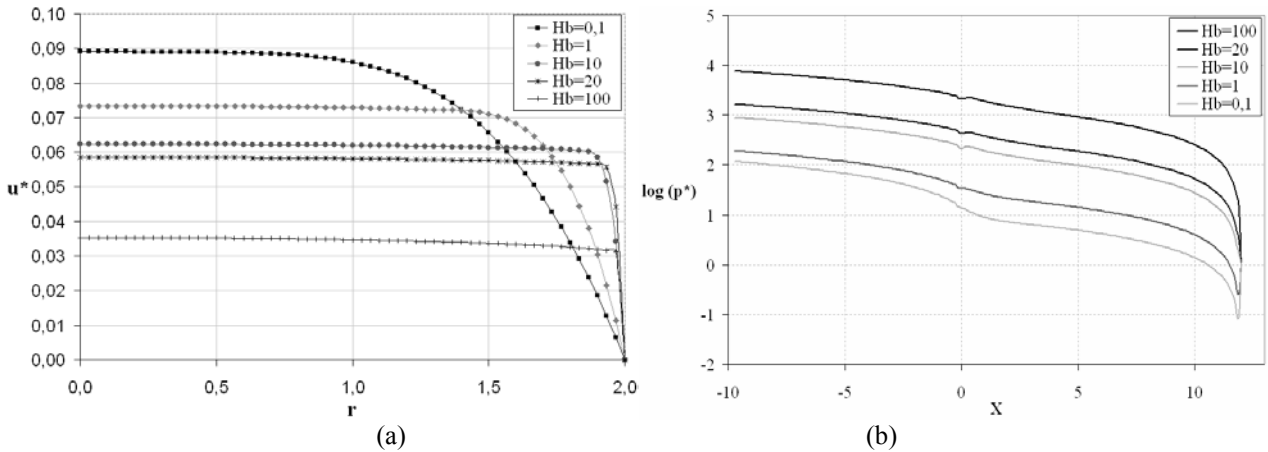


Figure 6. (a) Axial velocity profile of fully developed flow in  $x_1=10D_0$ . (b) Pressure drop along the symmetry axis.

In Fig. 7 we investigate how the decrease in the power-law index,  $n$ , from 1 to 0.2, affects the formation of the unyielded zones in the flow. These results of Fig. 8 correspond to  $Hb=0.1$ .

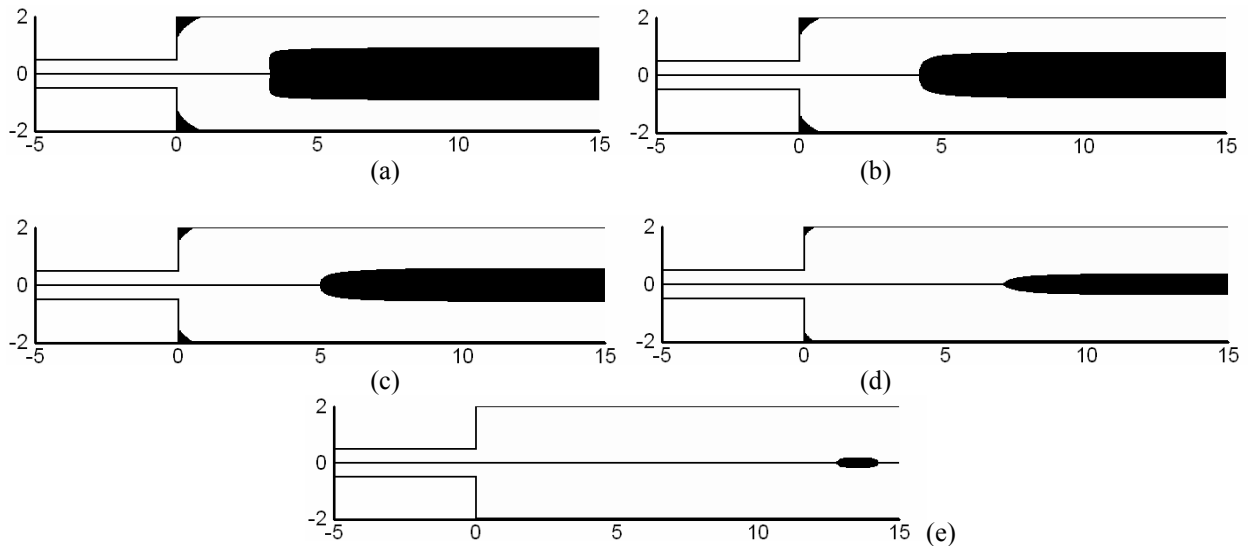


Figure 7. Yielded and unyielded regions, for  $Hb=0.1$ . (a)  $n=1$ , (b)  $n=0.8$ , (c)  $n=0.6$ , (d)  $n=0.37$ , (e)  $n=0.2$ .

We observe that, as  $n$  decreases, the size of the unyielded zones also decreases and are pushed downstream farther from the expansion. These results are in agreement with the literature (Jay et al., 2001). This behavior is due to fluid's shear-thinning, which goes against the viscosity increase tendency in the low shear rate range, preventing the fluid's plasticization.

In Figs. 8 and 9, a more detailed study the influence of the power-law index the corner of the expansion was performed, for  $n=0.8$  and  $n=0.37$ , and several values of  $Hb$ . We observe that, for  $n=0.8$  the unyielded structure that is formed as the  $Hb$  increases prevents the formation of a vortex, as it has been noted in previous works (Jay et. al, 2001, Zinani and Frey, 2006). For  $n=0.37$ , a vortex was not detected. In both cases, the increase of the  $Hb$  increased the size of the unyielded zone.

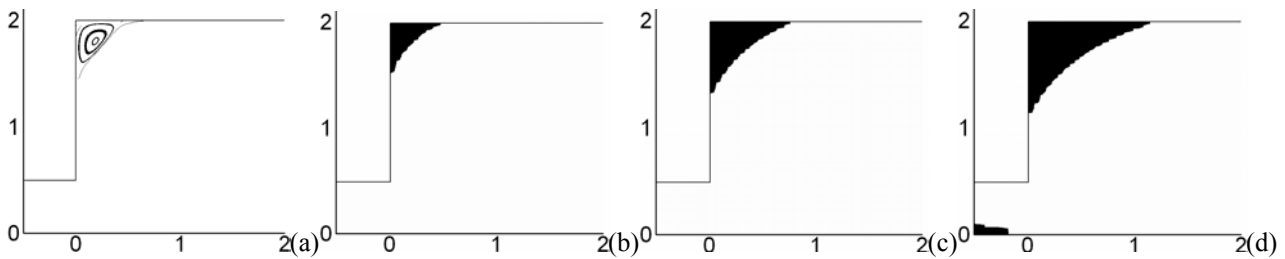


Figure 8. Yielded regions,  $n=0.8$  (a)  $Hb=0$ , (b)  $Hb=0.05$ , (c)  $Hb=0.1$  and (d)  $Hb=1$ .

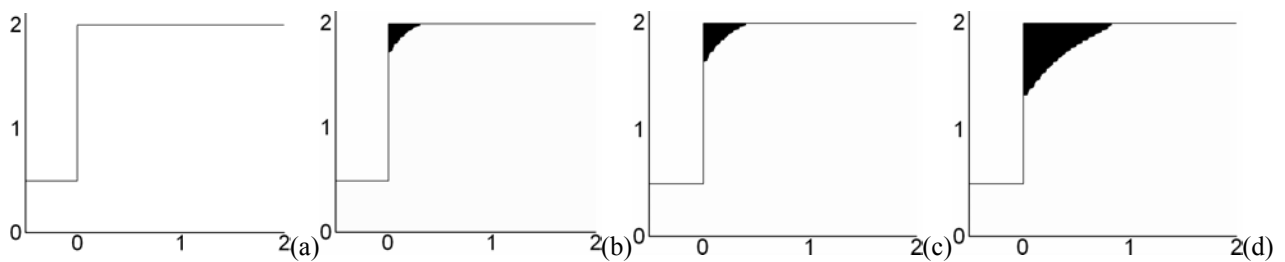


Figure 9. Yielded regions,  $n=0.37$  (a)  $Hb=0$ , (b)  $Hb=0.05$ , (c)  $Hb=0.1$  and (d)  $Hb=1$ .

In Fig. 10 we present a comparison of our results for  $n=0.37$  and (a)  $Hb=1$ , (b)  $Hb=100$ . The dots correspond to Jay et al. results and the filled lines to ours. In the corner, the yield surfaces are quite similar, but in the plug-flow along the symmetry axis, they look quite different. Our results tend to predict a much greater unyielded region. As this work is still in progress, a more detailed analysis will be performed, perhaps varying the regularization parameter  $a$ , in order to find out about these discrepancies, but attempting to the fact that the mesh employed herein is much more refined than that of Jay et. al (2001).

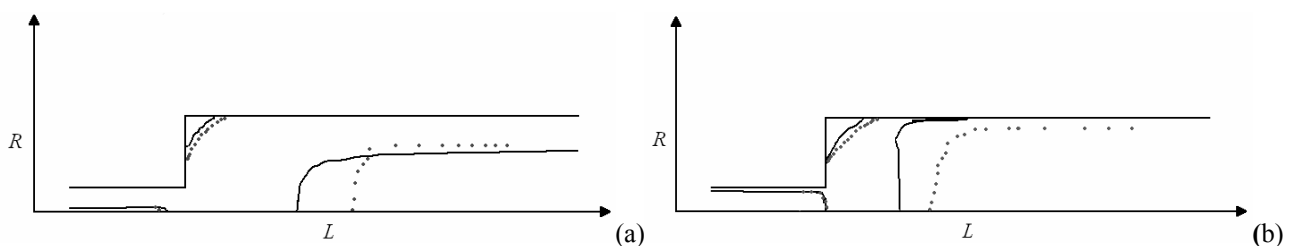


Figure 10. Comparison with results of Jay et. al, 2001, for  $n=0.37$  and (a)  $Hb=1$ , (b)  $Hb=100$ .

## 5. FINAL REMARKS

We implemented a GLS formulation for the approximation of flows of Newtonian and viscoplastic liquids. The Newtonian results were compared with the literature and a good agreement was found. The features of Herschel-Bulkley fluids flowing through an axisymmetric expansion were investigated. For the same Reynolds number and power-law index, unyielded zones were greater for fluids with higher yield stress. For the same Reynolds and Herschel-Bulkley number, the more shear-thinning fluids presented smaller unyielded regions. The more viscoplastic fluids case a higher pressure drop in the flows due to the rigid unyielded plug-plow region that is formed along the symmetry axis. The unyielded zones, when compared with other authors, were always greater in this work, despite they were quite similar. This feature deserves a deeper investigation and is the subject of a future work, in which the influence of the Papanastasiou regularization parameter will be investigated and more comparisons will be performed.

## 6. ACKNOWLEDGEMENTS

The author F. Machado thanks the agency CAPES/Brazil for the master's grant. The author F. Zinani thanks MCT/CNPq (Proc. 154619/2006-0) for the post doctoral grant. The author and S. Frey thanks MCT/CNPq grant No.



50747/1993-8. We also acknowledge MCT/CNPq for the financial support provided by projects of Proc. 477063/2004-7 and Proc. 472094/2006-8.

## 7. REFERENCES

- Alexandrou, A. N., McGilvrey, T. M., and Burgos, G., 2001. "Steady Herschel-Bulkley fluid in tree-dimensional expansions", *J. Non-Newt. Fluid Mech.*, vol. 100, pp. 77-96.
- Bird R. B, Armstrong R. C., Hassager, O., 1987. "Dynamics of polymeric liquids, Vol. 1, Fluid Dynamics". John Wiley and Sons, New York, pp. 649.
- Brooks, A.N., Hughes, T.J.R., 1982, "Streamline Upwind/Petrov-Galerkin Formulations for Convective Dominated Flows with Particular Emphasis on the Incompressible Navier-Stokes Equations", *Computer Methods in Applied Mechanics and Engineering*, **32**, p. 199-259.
- Burgos, G., Alexandrou, A. N., and Entov, V., 1999. "On the determination of yield surfaces in Herschel-Bulkley fluids", *J. of Rheology*, vol. 43 (3), pp. 463-483.
- Ciarlet, P.G., 1978, *The Finite Element Method for Elliptic Problems*, North-Holland, Amsterdam, pp. 530.
- Franca, L.P., and Frey, S., 1992. "Stabilized finite element methods: II. The incompressible Navier-Stokes equations", *Comput. Methods Appl. Mech. Engrg.*, vol. 99, pp. 209-233.
- Gurtin, M.E., 1981. "An introduction to continuum mechanics", Academic Press, New York, pp. 265.
- Hughes, T.J.R., Franca, L.P., Balestra, M., 1986, "A New Finite Element Formulation for Computational Fluid Dynamics: V. Circumventing the Babuška-Brezzi Condition: A Stable Petrov-Galerkin Formulation of the Stokes Problem Accommodating Equal-Order Interpolations". *Computer Methods in Applied Mechanics and Engineering*, **59**, pp. 85-99.
- Lipscomb, G. G., Denn, M. M., 1984: "Flow of Bingham fluids in complex geometries", *J. Non-Newtonian Fluid Mech.*, vol. 14, pp. 337-346.
- Macedo, A., P., 1995. "Aplicações de Métodos de Elementos Finitos Totalmente Estabilizados - GLS - à Simulação Numérica de escoamentos laminar e turbulentos". Dissertação de Mestrado, Universidade de Brasília, Brasília.
- Morgan, K., Periaux, J., and Thomasset, F., 1982. "Analysis of laminar flow over a Backward Facing Step". *A GAMM-Workshop*, Friedr. Vieweg & Sohn.
- Papanastasiou, T. C., 1987. "Flows of Materials with Yield", *J. of Rheology*, vol. 31 (5), pp. 385-404.
- Pascal, J., Magnin, A., and Piau, J. M., 2001. "Viscoplastic Fluid Flow Through a Sudden Axisymmetric Expansion", *AIChE Journal*, vol. 47, pp. 2155-2166.
- Slattery, J.C., 1999. "Advanced transport phenomena", Cambridge University Press, Cambridge.
- Schramm, G., 2006. "Reologia e Reometria - Fundamentos Teóricos e Práticos", Artliber Editora Ltda, Alemannha.
- Souza Mendes, P. R., Naccache, M. F., Vargas, P. R., and Marchesini, F. H., 2007. "Flow of viscoplastic liquids through axisymmetric expansions - contractions", *J. Non-Newt. Fluid Mech.*, vol. 142, pp. 207-217.
- Souza Mendes, P. R., and Dutra, E. S. S., 2004. "Viscosity Function for Yield-Stress Liquids", *Applied Rheology*, vol. 14, pp. 296-302.
- Zinani, F.; Frey, S.. Galerkin Least-Squares Finite Element Approximations for Isochoric Flows of Viscoplastic Liquids. *Journal of Fluids Engineering - Transactions of the Asme*, Estados Unidos, v. 128, n. 4, p. 856-863, 2006.

## 8. RESPONSIBILITY NOTICE

The authors are the only responsible for the printed material included in this paper.